JOURNAL OF MATERIALS RESEARCH AND TECHNOLOGY 2021;10:1184–1194

Available online at www.sciencedirect.com

jmr&t Journal of Materials Research and Technology

journal homepage: www.elsevier.com/locate/jmrt

Original Article

Performing regression-based methods on viscosity of nano-enhanced PCM - Using ANN and RSM

Nidal H. Abu-Hamdeh [a], **Ali Golmohammadzadeh** [b], **Aliakbar Karimipour** [c,*]

[a] Center of Research Excellence in Renewable Energy and Power Systems, Department of Mechanical Engineering, Faculty of Engineering, King Abdulaziz University, Jeddah 21589, Saudi Arabia
[b] Sapienza Università di Roma, Via Eudossiana 18, Roma, 00184, Italy
[c] Institute of Research and Development, Duy Tan University, Da Nang 550000, Viet Nam

ARTICLE INFO

Article history:
Received 10 September 2020
Accepted 11 December 2020
Available online 23 December 2020

Keywords:
MWCNT
Paraffin
Viscosity
Artificial neural network
Response surface method

ABSTRACT

Evaluation of the use of linear and nonlinear regression-based methods in estimating the viscosity of MWCNT/liquid paraffin nanofluid was investigated in this study. At temperature range of 5–65 °C, the viscosity of samples containing MWCNT nanoparticles at 0.005–5 wt.% which is measured by a Brookfield apparatus, was first evaluated to determine the response to the shear rate. The decrease in viscosity due to the increase in shear rate indicated that the rheological behavior of the nanofluid was non-Newtonian and therefore, in addition to temperature and mass fraction, the shear rate should be considered as an effective input parameter. Linear regression was performed by response surface methodology (RSM) and it was observed that the R-square for the best polynomial was 0.988. The results of nonlinear regression also showed that the neural network consisting of 3 and 13 neurons in the input and hidden layers was able to estimate the viscosity of the nanofluid more accurately so that the R-square value was calculated to be 0.998.

1. Introduction

Performance improvements can be found in buildings [1–3], solar collectors [4–8] heating and cooling [9–13], desalination [14–18] and heat exchangers [19]. Improvement in base fluid properties owing to loading nanoparticles has been introduced by researchers as a technique to improve usefulness [20–27]. Incorporation of nanoparticles into the base fluid modifies the thermophysical properties of the base fluid such that usually results in improved heat transfer [28–30]. Thermal conductivity of basic fluids such as water $\left(0.608\ \frac{W}{m.K}\right)$, ethylene glycol $\left(0.257\ \frac{W}{m.K}\right)$, and other base fluid is usually low [31]. Therefore, if the nanoparticles can be dispersed without settling in the base fluids, then the thermal conductivity of the base fluid can be expected to increase [32–34]. Phase change material are widely used by various researchers in applications such as energy storage [35], building [36,37] and

* Corresponding author.
E-mail address: aliakbarkarimipour@duytan.edu.vn (A. Karimipour).
https://doi.org/10.1016/j.jmrt.2020.12.040

electronic thermal management [38–40]. Paraffins have high latent heat and their benefits can be revealed during the phase change process. But PCM has a low thermal conductivity which results to a non-ideal phase process. By increasing the thermal conductivity, the phase change process can be improved. Considering the high thermal conductivity of MWCNT ($\sim 2000\ \frac{W}{m.K}$), many researchers utilized this material to prepare different nanofluid. Table 1 summarizes the applications of MWCNT in different nanofluids.

Paraffin has also been used as a base fluid by various researchers. Many studies have shown that analytical correlations are unable to estimate k_{nf} and μ_{nf} [54]. Usually, it is possible to estimate the thermophysical properties through the measurements of the experiment. But conducting many experimental tests are costly and time-consuming. One of the techniques for estimating the thermal conductivity as well as the viscosity of nanofluids is the utilizing of machine-based learning approaches [55]. In nanofluid scope, Machine-based learning is divided into MLP-ANN, GMDH, ANFIS, RBF and LSSVM methods. Afrand et al. [56] used the ANN method to estimate the viscosity of Fe/EG and found that applying ANN to estimate properties is very accurate, fast, and low-cost. Viscosity prediction of graphene nanosheets/water is performed by using ANN [57]. It was concluded that by applying ANN, the viscosity estimation is performed very precisely. Table 2 provides a summary of the applications of artificial neural networks in estimating the thermophysical properties of nanofluids.

According to Table 2, it is observed that the feasibility of using artificial neural network and RSM approaches to estimate the MWCNT/liquid paraffin viscosity has not been performed. In this study applying ANN and RSM approaches, the MWCNT/liquid paraffin viscosity at temperatures of 5–65 and 0–5 wt.% are estimated. Moreover, a correlation is proposed to estimate the nanofluid in terms of temperature, nanoparticle concentration and shear rate and finally, a comparison is made between the proposed correlation and the developed ANN.

2. Experimental data

Liu et al. [69] added MWCNTs nanoparticles to liquid paraffin to examine their effects on $\mu_{Paraffin}$. They provided many samples of nanofluids that have the requisite stability at 5–65°C and 0.005–5 wt.%. For this, zeta potential tests were performed and due to the reported critical value of zeta potential (−68 mV), the stability was acceptable. The results of the Brookfield DV-I PRIME digital viscometer are illustrated in Fig. 1. With the presence of MWCNT in the paraffin, non-Newtonian behavior was experienced (Fig. 2).

Fig. 2 reveals that $\frac{\mu_{MWCNT/Paraffin}}{\mu_{Paraffin}} > 1$ which means that $\mu_{MWCNT/Paraffin}$ is higher than $\mu_{Paraffin}$. Therefore the samples containing MWCNT have experienced more frictional force than the base fluid. At low shear rate ($\dot{\gamma}$), the value of $\frac{\mu_{MWCNT/Paraffin}}{\mu_{Paraffin}}$ is high. But considering the lower value for $\frac{\mu_{MWCNT/Paraffin}}{\mu_{Paraffin}}$ at higher $\dot{\gamma}$, it is concluded that as $\dot{\gamma}$ rises, nanoparticles have less effect on viscosity.

Table 1 – A summary on the nanofluid containing MWCNT.

Reference	Nanofluid	Concentration	Findings
Potschke et al. [41]	Adding MWCNTs to polycarbonate	Mass fraction up to 5%	up to 2 wt.%, Newtonian behavior
Yang et al. [42]	Adding MWCNT to oil dispersion	Mass fraction up to 0.3%	Non-Newtonian behavior
Esfe MH et al. [43]	MWCNTs-SiO_2/oil	Volume fraction up to 2%	up to 1 vol.%, Newtonian behavior
Seyhan et al. [44]	MWCNT/polyester	Mass fraction of 1%	Non-newtonian behavior
Yan et al. [24]	MWCNTs-TiO_2/EG	0.05-1 vol.%	Newtonian behavior
Esfe MH et al. [46]	ZnO-MWCNT/oil	Volume fraction of up to 1%	Newtonian
Dardan E et al. [47]	Incorporation of MWCNTs + Al_2O_3 to oil	Volume fraction up to 1%	Newtonian
Phuoc et al. [48]	Adding MWCNT to water	Volume fraction up to 1.5%	At 0.24 vol.% Newtonian while at 1.43 vol.% non-Newtonian behavior
Meng et al. [49]	MWCNT/EG	0.5–4 wt.%	Newtonian behavior
Eshgarf et al. [50]	SiO_2-MWCNTs/EG-Water	0.0625–2 vol.%	Non-Newtonian
Wang et al. [51]	MWCNT/DI water	0.05, 0.24,1.27 vol. %	Non-Newtonian
Ko et al. [52]	MWCNT/DI water	1.65 wt.%	Non-Newtonian
Nadooshan AA et al. [53]	SiO_2-MWCNTs/10 W40	0.05–1 vol.%	Non-Newtonian

Table 2 – Applications of Artificial Neural Network in nanofluids.

Reference	Nanofluid	Independent variable	Dependent variable	Findings
Esfe et al. [58]	FSWCNTs/EG	Temperature Volume fraction	$\frac{k_{nf}}{k_{bf}}$	R-square = 0.9998
Esfe et al. [59]	ZnO-DWCNT/EG	Temperature Volume fraction	$\frac{k_{nf}}{k_{bf}}$	R-square = 0.997
Esfe et al. [60]	ZnO-MWCNT/EG	Temperature Volume fraction	$\frac{k_{nf}}{k_{bf}}$	R-square = 0.9968
Esfe et al. [61]	CuO-MWCNT-10w40	Temperature Volume fraction Shear rate	μ	R-square = 0.9992 MSE = 1.81E−4.
Esfe et al. [62]	ZnO/10W40	Temperature Volume fraction Shear rate	$\frac{\mu_{nf}}{\mu_{bf}}$	R-square = 0.9999
Esfe et al. [63]	CuO/EG	Temperature Volume fraction	μ	R-square = 0.999 mean relative error = 0.0175.
Esfe et al. [64]	Al/oil	Temperature Volume fraction	μ k c_p $h_{convection}$	R-square = 0.9203 MSE = 2.167
Esfe et al. [65]	MWCNT and ZnO nanoparticles in 5W50	Temperature Volume fraction Shear rate	μ	R-square = 0.9999 MSE = 0.00003
Alirezaie et al. [66]	ofMWCNT (COOH-functionalized)/MgO - Engine oil	Temperature Volume fraction Shear rate	μ	R-square = 0.9973 MSE = 4.7352 E-6
Esfe et al. [67]	Al_2O_3-MWCNT-5W50	Temperature Volume fraction Shear rate	μ	R-square = 0.998 MSE = 5.1
Esfe et al. [68]	MWCNTs (10%) – Al_2O_3 (90%)/5W50	Temperature Volume fraction Shear rate	μ	R-square = 0.9998

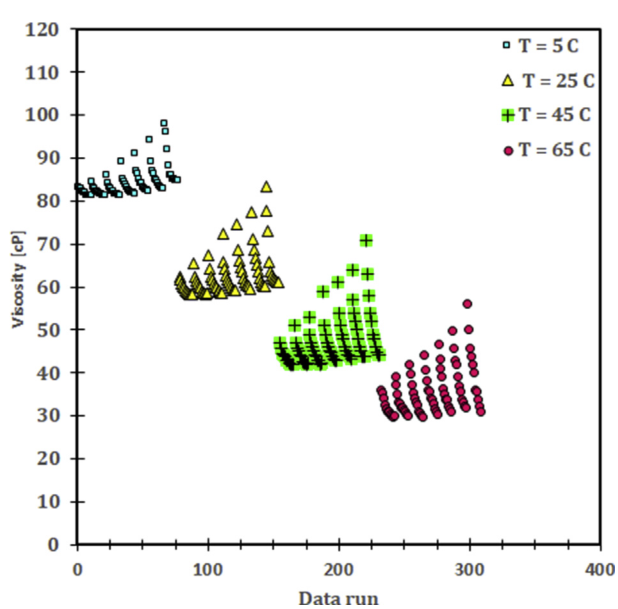

Fig. 1 – Liquid paraffin viscosity [69].

On the other hand, the intensity of non-Newtonian behavior depends on $\dot{\gamma}$. As $\dot{\gamma}$ increases, the rate of variation in viscosity diminishes (approaches to zero) which means that the viscosity no longer depend on $\dot{\gamma}$. In this case, the nanofluid experience Newtonian behavior. Focusing on Fig. 2 shows that at higher temperatures, the value of $\frac{\mu_{MWCNT/Paraffin}}{\mu_{Paraffin}}$ is higher and this shows that the presence of nanoparticles and their effect on viscosity intensifies with increasing temperature. The maximum viscosity increment was 86%, which was observed at $3\frac{1}{s}$ and 65.°C

3. ANN

The human brain is the most complex system ever observed and studied in the whole universe. But this sophisticated system has neither the size of a galaxy nor the number of components, more than modern-day supercomputers. The mysterious complexity of this unique system is due to the many connections it has between its components. Many types of research have been begun by computer scientists, engineers, and mathematicians, whose results are categorized in a branch of artificial intelligence and under the subcategory of computational intelligence as the topic of “artificial neural networks”. In the field of artificial neural networks, numerous mathematical and software models have been proposed to inspire the human brain, which are used to solve a wide range of scientific, engineering and practical problems in various fields.

Information enters the neuron through the inputs (as shown in Fig. 3). In the ANN model, each input is assigned a

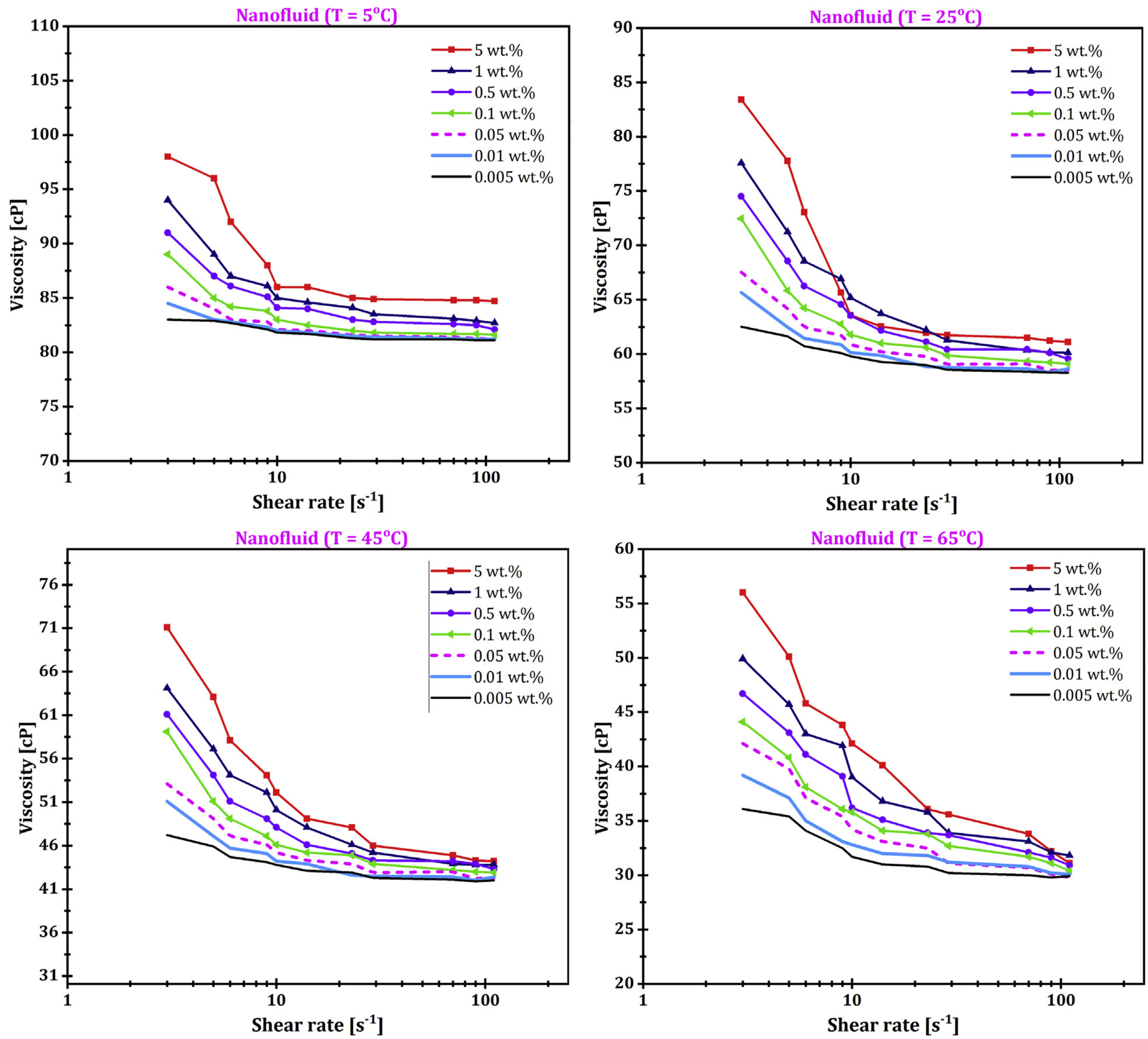

Fig. 2 – Nanofluid viscosity [69].

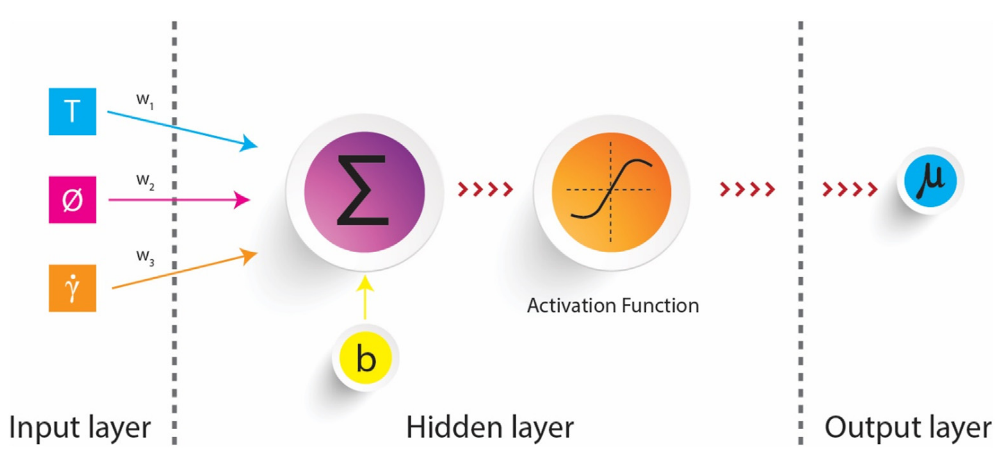

Fig. 3 – ANN structure.

Table 3 – P-value results.

Parameter	F -value	P -value	Parameter	F -value	P -value
T	655.15	<0.0001	$T\dot{\gamma}$	25.41	<0.0001
$\dot{\gamma}$	0.87	0.3511	$T\phi$	0.12	0.7297
ϕ	8.94	0.003	$\dot{\gamma}\phi$	41	<0.0001
T^2	201.07	<0.0001	$T\dot{\gamma}\phi$	3.89	0.049
$\dot{\gamma}^2$	183.34	<0.0001	$T^2\dot{\gamma}$	2.42	0.1209
ϕ^2	3.34	0.0685	$T^2\phi$	0.016	0.8985
T^3	1.92	0.1673	$T\dot{\gamma}^2$	7.46	0.0067
$\dot{\gamma}^3$	156	<0.0001	$T\phi^2$	2.64	0.1051
ϕ^3	9.38	0.0024	$\dot{\gamma}^2\phi$	33.05	<0.0001
			$\dot{\gamma}\phi^2$	21.09	<0.0001

According to Table 3, parameters of T, ϕ, $T\dot{\gamma}$, $\dot{\gamma}\phi$, T^2, $\dot{\gamma}^2$, $T\dot{\gamma}\phi$, $T\dot{\gamma}^2$, $\dot{\gamma}^2\phi$, $\dot{\gamma}\phi^2$, $\dot{\gamma}^3$, ϕ^3 are effective.

Table 4 – Coefficients value of the proposed correlation.

Parameter	Value	Parameter	Value
a_0	92.426	a_7	−1.74519E-004
a_1	−1.26201	a_8	1.76246E-005
a_2	12.10735	a_9	4.91721E-004
a_3	−3.50984E-003	a_{10}	0.010787
a_4	−0.11672	a_{11}	−5.47522E-005
a_5	9.05104E-003	a_{12}	1.03633
a_6	0.010092		

weight (wi). These weights are actually the importance of inputs, meaning the more weights, the more important the input for network training. Then all inputs are assembled and inserted into the axon in a single layer. Next, the activation function applies to the data. The activation function is defined as the type of neural network in which it contains a mathematical formula for updating weights in the network. After computing at this stage, the information enters the other neurons through the output synapses, and this stage continues until the network is trained. The number of prerequisite neurons in the input layer depends on the number of input variables and since the input variables include T, ϕ, $\dot{\gamma}$

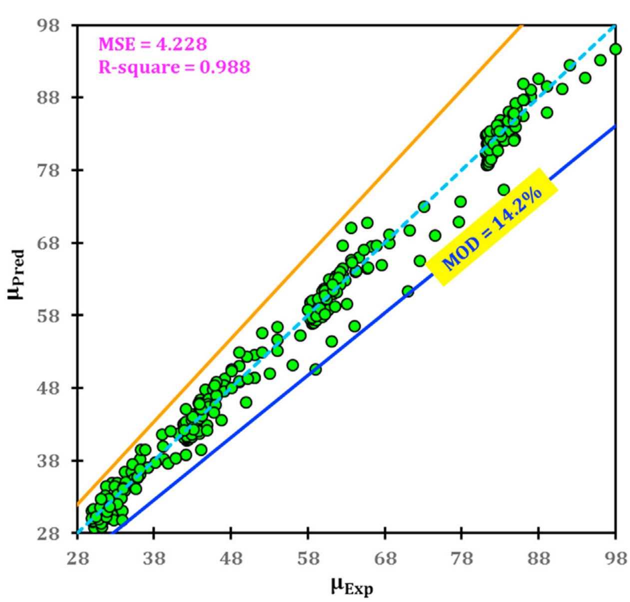

Fig. 4 – The margin of deviation for RSM method (Eq. (4)).

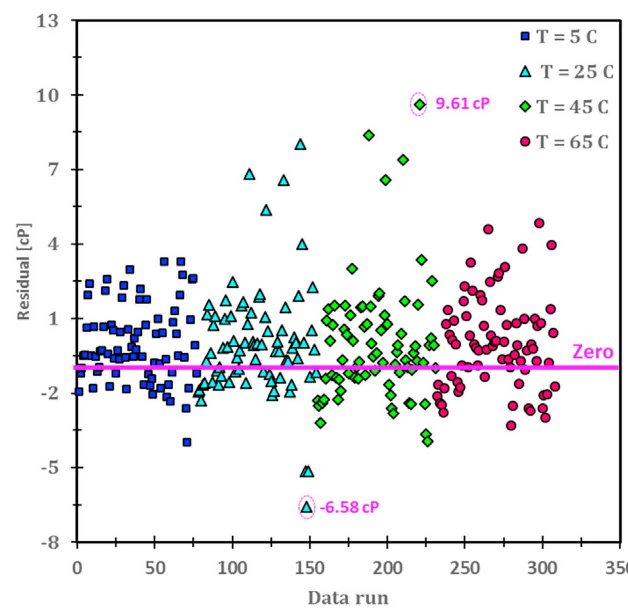

Fig. 5 – Residual value for the proposed correlation (RSM).

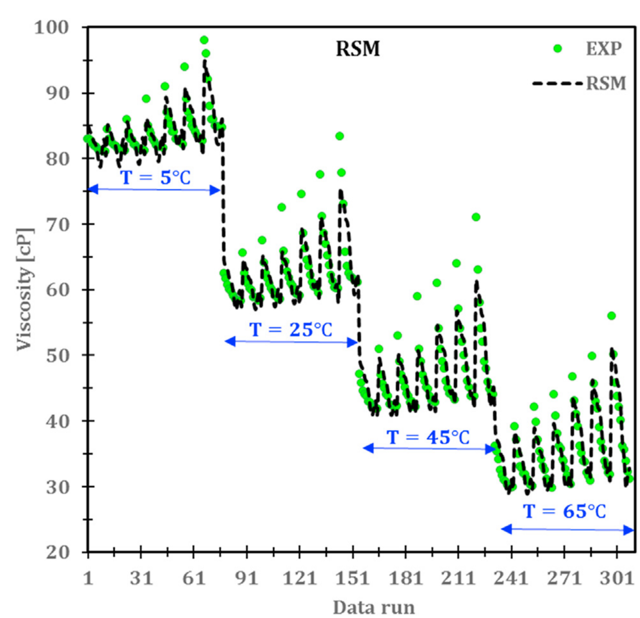

Fig. 6 – Comparsion between the experimental and outputs of the proposed correlations.

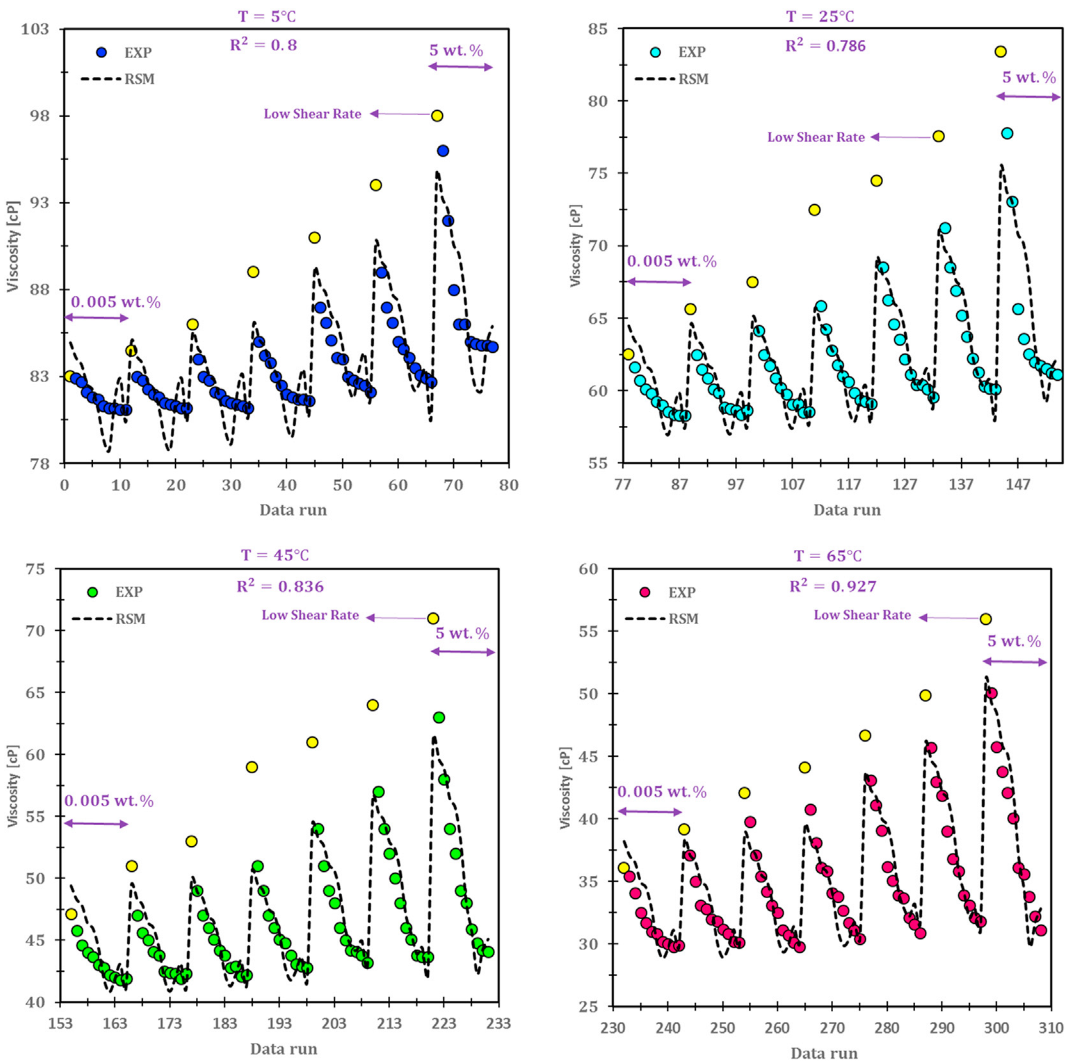

Fig. 7 – Results derived from RSM technique and its comparison with experimental ones.

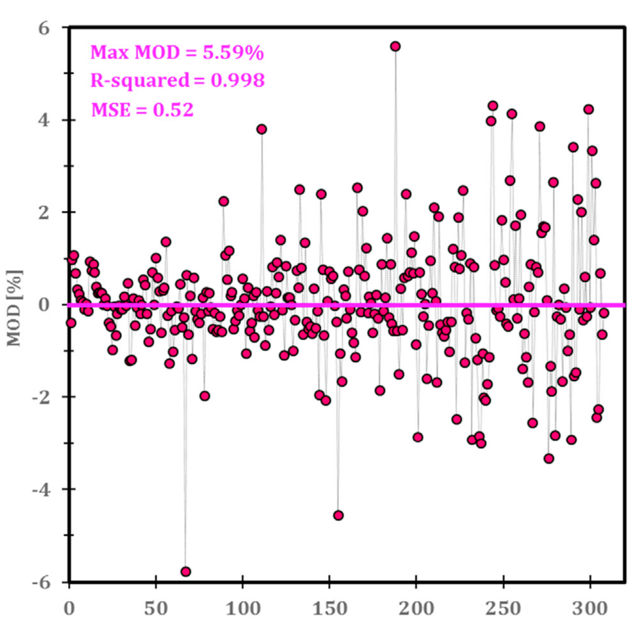

Fig. 8 – Margin of deviation for ANN technique.

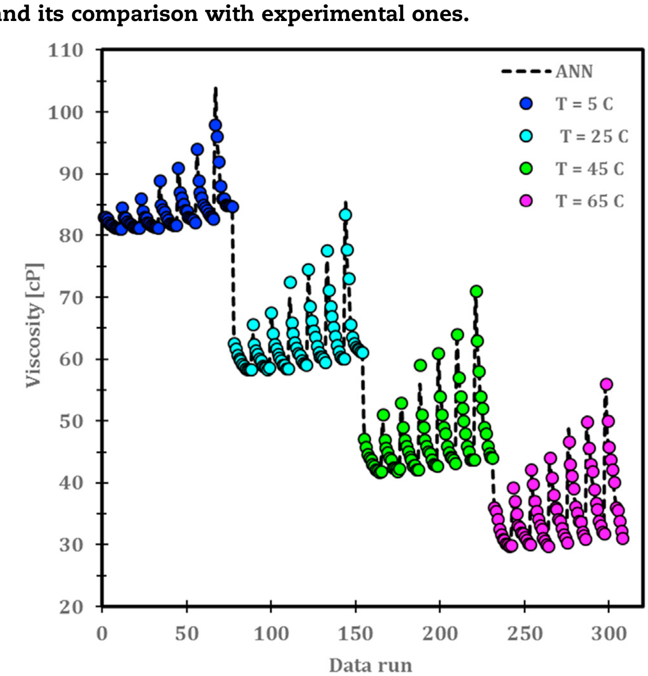

Fig. 9 – Comparison between the experimental and outputs of the ANN.

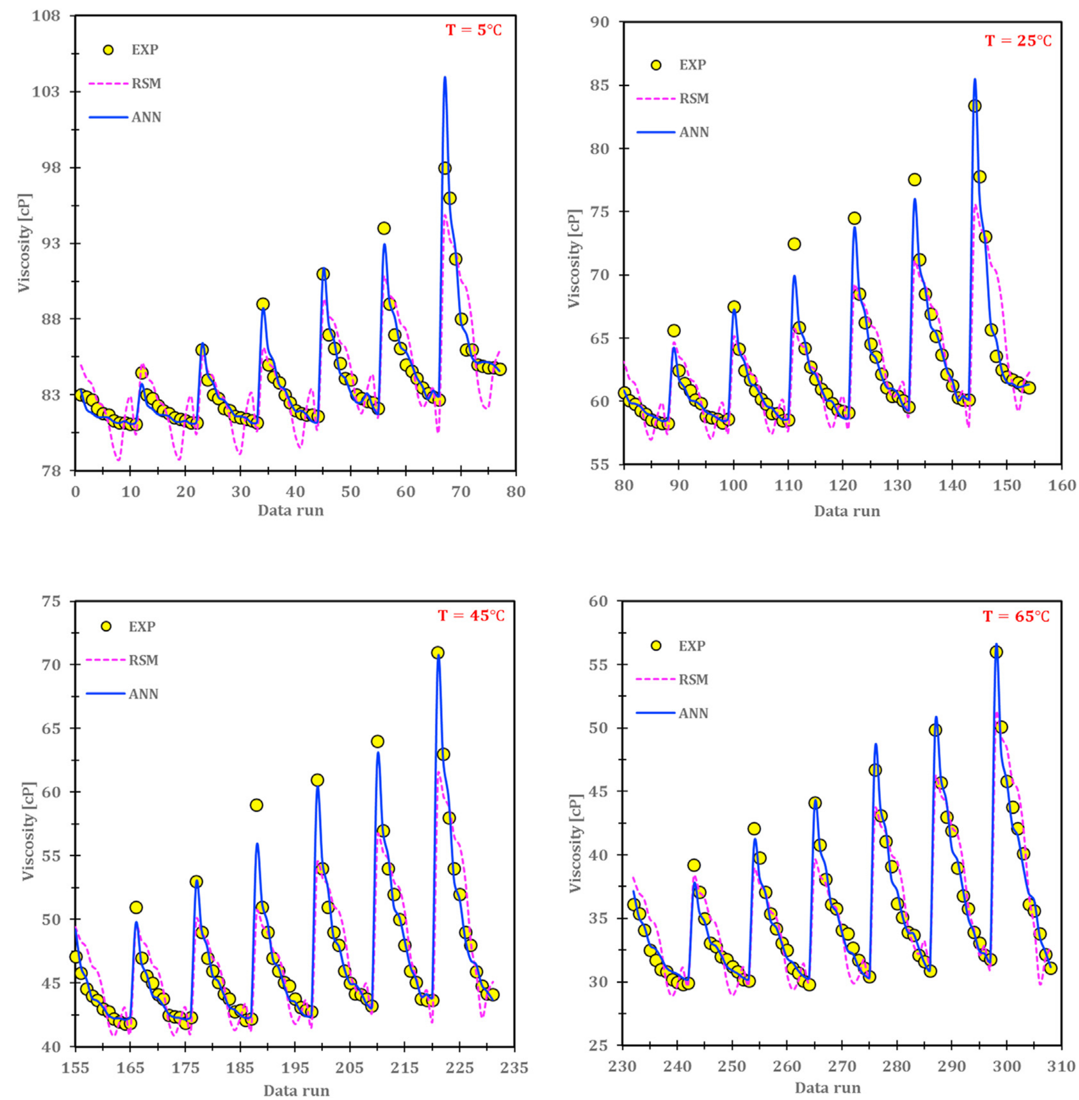

Fig. 10 – Comparison between ANN and RSM techniques.

(Fig. 3), three neurons are assigned to the input layer. The number of output neurons also depends on the number of target parameters and since in this study, viscosity is the only output, hence only one neuron is assigned to the output layer. The number of neurons in the hidden layer is also subject to trial and error.

4. Response surface methodology (RSM)

RSM technique attempts to evaluate the viscosity (output variable) behavior with respect to the input variables $(T,\phi,\dot{\gamma})$by presenting a polynomial function. Three models of linear, quadratic and cubic are used in this method. In the linear model, there are certain term such as T, $\phi$and $\dot{\gamma}$, whereas in the quadratic model in addition to the mentioned parameters, other parameters are there such as $T\phi$, $T\dot{\gamma}$, $\phi\dot{\gamma}$, T^2, ϕ^2, $\dot{\gamma}^2$. However in the cubic model, in addition to the above parameters, some parameters such as $T\dot{\gamma}\phi, T\dot{\gamma}^2, T\phi^2, T^2\dot{\gamma}, \phi^2\dot{\gamma}, \dot{\gamma}^2\phi, T^3$, ϕ^3, $\dot{\gamma}^3$are there. Applying analysis of variance (ANOVA), the best model is selected from linear, quadratic and cubic polynomials. Then, performing P-value, the significance of each parameter can be evaluated. In ANN and RAM methods, mean square error (Eq. 1) and R-sqaure (Eq. 2) are examined to select the best algorithm and polynomial. In this study, more R-square and less mean square error (MSE) are more desirable.

$$MSE = \frac{1}{N}\sum_{i=1}^{N}\left(\mu_{Pred} - \mu_{Exp}\right)^2 \tag{1}$$

$$R - square = \left(\frac{\sum_{i=1}^{N}\left(\mu_{Exp} - \overline{\mu}_{exp}\right)\left(\mu_{Pred} - \overline{\mu}_{Pred}\right)}{\sqrt[2]{\sum_{i=1}^{N}\left(\mu_{Exp} - \overline{\mu}_{exp}\right)^2}\ \sqrt[2]{\sum_{i=1}^{N}\left(\mu_{Pred} - \overline{\mu}_{Pred}\right)^2}}\right)^2 \tag{2}$$

5. Results and discussion

To estimate the MWCNT-liquid paraffin nanofluid viscosity, the linear, quadratic and cubic polynomials were examined. Given the constraint of maximizing the R-squared, a cubic model was chosen.

$$\mu_{nf} = b_0 + b_1 T + b_2 \phi + b_3\dot{\gamma} + b_4 T\phi + b_5 T\dot{\gamma} + b_6\phi\dot{\gamma} + b_7 T^2 + b_8 \phi^2 + b_9\dot{\gamma}^2 + b_{10}T\phi\dot{\gamma} + b_{11}T^2\phi + b_{12}T^2\dot{\gamma} + b_{13}T\phi^2 + b_{14}T\dot{\gamma}^2 + b_{15}\phi^2\dot{\gamma} + b_{16}\dot{\gamma}^2\phi + b_{17}T^3 + b_{18}\phi^3 + b_{19}\dot{\gamma}^3 \tag{3}$$

Now the question must be answered whether all the terms in Eq. (3) are of high importance? Are there terms that are not important and can be eliminated? The significance of each term is evaluated through performing the probability test (p-value) so that if the p-value is greater than 0.1, the term can be omitted. By another criterion, the parameters in which the p-value is less than 0.05 are important and the other parameters will be deleted. The p-value test results can be found in Table 3.

Therefore, Eq. (3) is rewritten as follows:

$$\mu_{nf} = a_0 + a_1 T + a_2 \phi + a_3 T\dot{\gamma} + a_4 \dot{\gamma}\phi + a_5 T^2 + a_6\dot{\gamma}^2 + a_7 T\dot{\gamma}\phi + a_8 T\dot{\gamma}^2 + a_9\dot{\gamma}^2\phi + a_{10}\dot{\gamma}\phi^2 + a_{11}\dot{\gamma}^3 + a_{12}\phi^3 \tag{4}$$

The values of the coefficients in Eq. (4) are reported in Table 4.

Based on Eqs. (1) and (2), MSE and R-square are 4.228 and 0.988, respectively. High R-squared of 0.988 indicates acceptable viscosity prediction ability of the correlation. The margin of deviation (MOD) in Fig. 4 can be obtained from the following equation:

$$MOD = \left|\frac{\mu_{Exp} - \mu_{Pred}}{\mu_{Exp}}\right| \times 100 \tag{5}$$

According to Eq. (5), calculations show that the maximum MOD is 14.42%.

The residual is obtained by subtracting the experimental and predicted data. The distribution of residual is plotted in Fig. 5. If the residual value for more points is close to the zero line, it means that the accuracy of the correlation is higher.

By plotting the experimental data and comparing it with the predicted results, one can observe the ability of correlation for viscosity estimation. Fig. 6 evaluate the correlation ability for the prediction of viscosity of MWCNT/paraffin. In Fig. 7, the comparison was made at each temperature. Also, the R-square value was documented at each temperature.

It is almost possible that as the temperature rises, the accuracy of the correlation in the viscosity prediction becomes better. On the other hand, by focusing more on Fig. 7, we can see that at any temperature, the lowest correlation accuracy occurs at low shear rates. Eventually, it is concluded that the correlation accuracy is enhanced by increasing the temperature and shear rate.

Now the results of the artificial neural network are examined. The results show that if the number of hidden layer neurons to be 13, the trained neural network will be the best. Note that the best case corresponds to the highest R-squared and the lowest mean square error. Fig. 8 shows the MOD variation for the neural network. As shown, the maximum value of MOD is 5.59%.

Fig. 9 shows the comparison between the experimental results and the values estimated by the ANN. As can be seen, the neural network accurately predicts and trend the viscosity variations.

The values of R-squared and MSE are also shown in Fig. 8. The value of R-squares in the neural network is equal to 0.998, which is higher than the corresponding value in the RSM method (0.988) and is superior in this respect. A comparison between MSE in the ANN (0.52) and RSM (4.228) techniques reveals that the ANN is also superior in this respect. Finally, the predictive power of both approaches is compared in Fig. 10. This comparison demonstrates that the accuracy of the ANN is far better than the RSM method.

6. Conclusion

In this study, the MWCNT-liquid paraffin nanofluid viscosity was evaluated numerically through applying artificial neural (ANN) network and response surface method (RSM) techniques. Owing to non-Newtonian behavior of the MWCNT-liquid paraffin, three variables of temperature, shear rate and mass fraction were introduced into the RSM and ANN algorithms as inputs at 5–65°C, 3–110 $\frac{1}{s}$ and 0.005–5 wt.% (308 points). Results showed that the response surface cubic model can accurately estimate the viscosity of MWCNT-liquid paraffin. The ANOVA analysis for the developed cubic model showed that the R-square value was 0.988, while the mean square error was 4.228. Moreover, the maximum margin of deviation for the developed cubic model was 14.2%. Artificial neural network technique calculations showed that the network with thirteen neurons has priority over other cases. The R-square value in this technique was calculated to be 0.998 and the mean square error was 0.52. Moreover, the maximum margin of deviation for the developed ANN was 5.59%. Finally, a comparison between ANN and RSM techniques exhibited that the ANN technique is more precise than the RSM for navigating the viscosity field.

Declaration of Competing Interest

There is no conflict of interest.

Acknowledgment

The Deanship of Scientific Research (DSR) at King Abdulaziz University, Jeddah, Saudi Arabia funded this project, under grant no. (FP-203-42).

REFERENCES

[1] Rostami S, et al. A review of melting and freezing processes of PCM/Nano-PCM and their application in energy storage.

Energy 2020:118698. https://doi.org/10.1016/j.energy.2020.118698. 08/27/2020.

[2] Ma YX, Yu C. Impact of meteorological factors on high-rise office building energy consumption in Hong Kong: From a spatiotemporal perspective. Energy Build 2020;228:110468. https://doi.org/10.1007/s10973-020-09713-9. 04/23/2020.

[3] Nariman A, Kalbasi R, Rostami S. Sensitivity of AHU power consumption to PCM implementation in the wall-considering the solar radiation. J Therm Anal Calorim 2020. https://doi.org/10.1007/s10973-020-10068-4. 08/03 2020.

[4] Alsagri AS. Design and dynamic simulation of a photovoltaic thermal-organic Rankine cycle considering heat transfer between components. Energy Convers Manag 2020;225:113435.

[5] Alsagri AS. Energy performance enhancement of solar thermal power plants by solar parabolic trough collectors and evacuated tube collectors-based preheating units. Int J Energy Res 2020. https://doi.org/10.1002/er.5431.

[6] Bezaatpour M, Rostamzadeh H, Bezaatpour J. Hybridization of rotary absorber tube and magnetic field inducer with nanofluid for performance enhancement of parabolic trough solar collector. J Clean Prod 2020:124565. https://doi.org/10.1016/j.jclepro.2020.124565.

[7] Yang L, Du K. Thermo-economic analysis of a novel parabolic trough solar collector equipped with preheating system and canopy. Energy 2020;211:118900.

[8] Mohammed RH, Alsagri AS, Wang X. Performance improvement of supercritical carbon dioxide power cycles through its integration with bottoming heat recovery cycles and advanced heat exchanger design: a review. Int J Energy Res 2020. https://doi.org/10.1002/er.5319.

[9] Kalbasi R, Ruhani B, Rostami S. Energetic analysis of an air handling unit combined with enthalpy air-to-air heat exchanger. J Therm Anal Calorim 2020;139(4):2881–90. https://doi.org/10.1007/s10973-019-09158-9. 02/01 2020.

[10] Liu W, Kalbasi R, Afrand M. Solutions for enhancement of energy and exergy efficiencies in air handling units. J Clean Prod 2020;257:120565. https://doi.org/10.1016/j.jclepro.2020.120565. 06/01/2020.

[11] Shahsavar Goldanlou A, Kalbasi R, Afrand M. Energy usage reduction in an air handling unit by incorporating two heat recovery units. J Build Eng 2020;32:101545. https://doi.org/10.1016/j.jobe.2020.101545. 11/01/2020.

[12] Kalbasi R, Shahsavar A, Afrand M. Incorporating novel heat recovery units into an AHU for energy demand reduction-exergy analysis. J Therm Anal Calorim 2020;139(4):2821–30. https://doi.org/10.1007/s10973-019-09060-4. 02/01 2020.

[13] Kalbasi R, Shahsavar A, Afrand M. Reducing AHU energy consumption by a new layout of using heat recovery units. J Therm Anal Calorim 2020;139(4):2811–20. https://doi.org/10.1007/s10973-019-09070-2. 02/01 2020.

[14] Parsa SM, et al. Experimental investigation at a summit above 13,000ft on active solar still water purification powered by photovoltaic: a comparative study. Desalination 2020;476:114146. https://doi.org/10.1016/j.desal.2019.114146. 02/15/2020.

[15] Parsa SM, Rahbar A, Javadi Y D, Koleini MH, Afrand M, Amidpour M. Energy-matrices, exergy, economic, environmental, exergoeconomic, enviroeconomic, and heat transfer (6E/HT) analysis of two passive/active solar still water desalination nearly 4000m: altitude concept. J Clean Prod 2020;261:121243. https://doi.org/10.1016/j.jclepro.2020.121243. 07/10/2020.

[16] Afrand M, Kalbasi R, Karimipour A, Wongwises S. Experimental investigation on a thermal model for a basin solar still with an external reflector. Energies 2017;10(1):18.

[17] Parsa SM, Rahbar A, Koleini MH, Aberoumand S, Afrand M, Amidpour M. A renewable energy-driven thermoelectric-utilized solar still with external condenser loaded by silver/nanofluid for simultaneously water disinfection and desalination. Desalination 2020;480:114354. https://doi.org/10.1016/j.desal.2020.114354. 04/15/2020.

[18] Parsa SM, et al. First approach on nanofluid-based solar still in high altitude for water desalination and solar water disinfection (SODIS). Desalination 2020;491:114592. https://doi.org/10.1016/j.desal.2020.114592. 10/01/2020.

[19] Ahmadi Nadooshan A, Kalbasi R, Afrand M. Perforated fins effect on the heat transfer rate from a circular tube by using wind tunnel: an experimental view. Heat Mass Tran 2018;54(10):3047–57. https://doi.org/10.1007/s00231-018-2333-3. 10/01 2018.

[20] Afrand M. Experimental study on thermal conductivity of ethylene glycol containing hybrid nano-additives and development of a new correlation. Appl Therm Eng 2017;110:1111–9.

[21] Esfe MH, Rostamian H, Esfandeh S, Afrand M. Modeling and prediction of rheological behavior of Al2O3-MWCNT/5W50 hybrid nano-lubricant by artificial neural network using experimental data. Phys Stat Mech Appl 2018;510:625–34.

[22] Ghaffarkhah A, et al. On evaluation of thermophysical properties of transformer oil-based nanofluids: a comprehensive modeling and experimental study. J Mol Liq 2020;300:112249.

[23] Moradikazerouni A, Hajizadeh A, Safaei MR, Afrand M, Yarmand H, Zulkifli NWBM. Assessment of thermal conductivity enhancement of nano-antifreeze containing single-walled carbon nanotubes: optimal artificial neural network and curve-fitting. Phys Stat Mech Appl 2019;521:138–45.

[24] Yan S-R, Kalbasi R, Nguyen Q, Karimipour A. Rheological behavior of hybrid MWCNTs-TiO2/EG nanofluid: a comprehensive modeling and experimental study. J Mol Liq 2020;308:113058. https://doi.org/10.1016/j.molliq.2020.113058. 06/15/2020.

[25] Yan S-R, Kalbasi R, Karimipour A, Afrand M. Improving the thermal conductivity of paraffin by incorporating MWCNTs nanoparticles. J Therm Anal Calorim 2020. https://doi.org/10.1007/s10973-020-09819-0. 06/01 2020.

[26] Wei H, Afrand M, Kalbasi R, Ali HM, Heidarshenas B, Rostami S. The effect of tungsten trioxide nanoparticles on the thermal conductivity of ethylene glycol under different sonication durations: an experimental examination. Powder Technol 2020;374:462–9. https://doi.org/10.1016/j.powtec.2020.07.056. 09/01/2020.

[27] Tian X-X, Kalbasi R, Qi C, Karimipour A, Huang H-L. Efficacy of hybrid nano-powder presence on the thermal conductivity of the engine oil: an experimental study. Powder Technol 2020. https://doi.org/10.1016/j.powtec.2020.05.004. 05/05/2020.

[28] Pordanjani AH, Jahanbakhshi A, Nadooshan AA, Afrand M. Effect of two isothermal obstacles on the natural convection of nanofluid in the presence of magnetic field inside an enclosure with sinusoidal wall temperature distribution. Int J Heat Mass Tran 2018;121:565–78.

[29] Jafari K, Fatemi MH, Estelle P. Deep eutectic solvents (DESs): A short overview of the thermophysical properties and current use as base fluid for heat transfer nanofluids. Journal of Molecular Liquids 2021;321:114752.

[30] Vidhya R, Balakrishnan T, Suresh Kumar B. Investigation on thermophysical properties and heat transfer performance of heat pipe charged with binary mixture based ZnO-MgO hybrid nanofluids. Materials Today: Proceedings 2020. https://doi.org/10.1016/j.matpr.2020.09.284.

[31] Yang L, Ji W, Huang J-n, Xu G. An updated review on the influential parameters on thermal conductivity of nano-

fluids. J Mol Liq 2019;296:111780. https://doi.org/10.1016/j.molliq.2019.111780. 12/15/2019.
[32] Jebasingh Eanest, Arasu Valan. A comprehensive review on latent heat and thermal conductivity of nanoparticle dispersed phase change material for low-temperature applications. Energy Storage Materials 2020;24:52–74. https://doi.org/10.1016/j.ensm.2019.07.031.
[33] Ambreen Tehmina, Kim Man-Hoe. Influence of particle size on the effective thermal conductivity of nanofluids: A critical review. Applied Energy 2020;264:114684.
[34] Keyvani M, Afrand M, Toghraie D, Reiszadeh M. An experimental study on the thermal conductivity of cerium oxide/ethylene glycol nanofluid: developing a new correlation. J Mol Liq 2018;266:211–7.
[35] Liang Haobin, Niu Jianlei, Gan Yixiang. Performance optimization for shell-and-tube PCM thermal energy storage. J Energy Storage 2020;30:101421.
[36] Nurlybekova Gauhar, Memon Shazim Ali, Adilkhanova Indira. Quantitative evaluation of the thermal and energy performance of the PCM integrated building in the subtropical climate zone for current and future climate scenario. Energy 2021;219:119587. https://doi.org/10.1016/j.energy.2020.119587.
[37] Nurlybekova G, Memon SA, Adilkhanova I. Quantitative evaluation of the thermal and energy performance of the PCM integrated building in the subtropical climate zone for current and future climate scenario. Energy 2021;219:119587. https://doi.org/10.1016/j.energy.2020.119587.
[38] Ali HM, Arshad A. Experimental investigation of n-eicosane based circular pin-fin heat sinks for passive cooling of electronic devices. Int J Heat and Mass Tran 2017;112:649–61. https://doi.org/10.1016/j.ijheatmasstransfer.2017.05.004.
[39] Salimpour MR, Kalbasi R, Lorenzini G. Constructal multi-scale structure of PCM-based heat sinks. Continuum Mech Therm 2017;29(2):477–91. https://doi.org/10.1007/s00161-016-0541-y. 03/01 2017.
[40] Gharbi S, Harmand S, Jabrallah SB. Experimental comparison between different configurations of PCM based heat sinks for cooling electronic components. Appl Therm Eng 2015;87:454–62. https://doi.org/10.1016/j.applthermaleng.2015.05.024. 03/15/2019.
[41] Pötschke P, Fornes TD, Paul DR. Rheological behavior of multiwalled carbon nanotube/polycarbonate composites. Polymer 2002;43(11):3247–55. https://doi.org/10.1016/S0032-3861(02)00151-9. 05/01/2002.
[42] Yang Y, Grulke EA, Zhang ZG, Wu G. Thermal and rheological properties of carbon nanotube-in-oil dispersions. J Appl Phys 2006;99(11):114307. https://doi.org/10.1063/1.2193161.
[43] Esfe MH, Afrand M, Yan W-M, Yarmand H, Toghraie D, Dahari M. Effects of temperature and concentration on rheological behavior of MWCNTs/SiO2 (20–80)-SAE40 hybrid nano-lubricant. Int Commun Heat Mass Tran 2016;76:133–8.
[44] Seyhan AT, Gojny FH, Tanoğlu M, Schulte K. Rheological and dynamic-mechanical behavior of carbon nanotube/vinyl ester–polyester suspensions and their nanocomposites. Eur Polym J 2007;43(7):2836–47. https://doi.org/10.1016/j.eurpolymj.2007.04.022. 07/01/2007.
[46] Esfe MH, Afrand M, Rostamian SH, Toghraie D. Examination of rheological behavior of MWCNTs/ZnO-SAE40 hybrid nano-lubricants under various temperatures and solid volume fractions. Exp Therm Fluid Sci 2017;80:384–90.
[47] Dardan E, Afrand M, Meghdadi Isfahani AH. Effect of suspending hybrid nano-additives on rheological behavior of engine oil and pumping power. Appl Therm Eng 2016;109:524–34. https://doi.org/10.1016/j.applthermaleng.2016.08.103. 10/25/2016.
[48] Phuoc TX, Massoudi M, Chen R-H. Viscosity and thermal conductivity of nanofluids containing multi-walled carbon nanotubes stabilized by chitosan. Int J Therm Sci 2011;50(1):12–8. https://doi.org/10.1016/j.ijthermalsci.2010.09.008. 01/01/2011.
[49] Meng Z, Wu D, Wang L, Zhu H, Li Q. Carbon nanotube glycol nanofluids: photo-thermal properties, thermal conductivities and rheological behavior. Particuology 2012;10(5):614–8. https://doi.org/10.1016/j.partic.2012.04.001. 10/01/2012.
[50] Eshgarf H, Afrand M. An experimental study on rheological behavior of non-Newtonian hybrid nano-coolant for application in cooling and heating systems. Exp Therm Fluid Sci 2016;76:221–7. https://doi.org/10.1016/j.expthermflusci.2016.03.015. 09/01/2016.
[51] Wang J, Zhu J, Zhang X, Chen Y. Heat transfer and pressure drop of nanofluids containing carbon nanotubes in laminar flows. Exp Therm Fluid Sci 2013;44:716–21. https://doi.org/10.1016/j.expthermflusci.2012.09.013. 01/01/2013.
[52] Ko GH, et al. An experimental study on the pressure drop of nanofluids containing carbon nanotubes in a horizontal tube. Int J Heat Mass Tran 2007;50(23):4749–53. https://doi.org/10.1016/j.ijheatmasstransfer.2007.03.029. 11/01/2007.
[53] Nadooshan AA, Esfe MH, Afrand M. Evaluation of rheological behavior of 10W40 lubricant containing hybrid nano-material by measuring dynamic viscosity. Phys E Low-dimens Syst Nanostruct 2017;92:47–54.
[54] Saidur R, Kazi SN, Hossain MS, Rahman MM, Mohammad HA. A review on the performance of nanoparticles suspended with refrigerants and lubricating oils in refrigeration systems. Renew Sustain Energy Rev 2011;15(1):310–23. https://doi.org/10.1016/j.rser.2010.08.018.
[55] Ramezanizadeh M, Ahmadi MH, Nazari MA, Sadeghzadeh M, Chen L. A review on the utilized machine learning approaches for modeling the dynamic viscosity of nanofluids. Renew Sustain Energy Rev 2019;114:109345. https://doi.org/10.1016/j.rser.2019.109345. 10/01/2019.
[56] Afrand M, Ahmadi Nadooshan A, Hassani M, Yarmand H, Dahari M. Predicting the viscosity of multi-walled carbon nanotubes/water nanofluid by developing an optimal artificial neural network based on experimental data. Int Commun Heat Mass Tran 2016;77:49–53. https://doi.org/10.1016/j.icheatmasstransfer.2016.07.008. 10/01/2016.
[57] Vakili M, Khosrojerdi S, Aghajannezhad P, Yahyaei M. A hybrid artificial neural network-genetic algorithm modeling approach for viscosity estimation of graphene nanoplatelets nanofluid using experimental data. Int Commun Heat Mass Tran 2017;82:40–8. https://doi.org/10.1016/j.icheatmasstransfer.2017.02.003. 03/01/2017.
[58] Hemmat Esfe M, Firouzi M, Afrand M. Experimental and theoretical investigation of thermal conductivity of ethylene glycol containing functionalized single walled carbon nanotubes. Phys E Low-dimens Syst Nanostruct 2018;95:71–7. https://doi.org/10.1016/j.physe.2017.08.017. 01/01/2018.
[59] Esfe MH, Esfandeh S, Afrand M, Rejvani M, Rostamian SH. Experimental evaluation, new correlation proposing and ANN modeling of thermal properties of EG based hybrid nanofluid containing ZnO-DWCNT nanoparticles for internal combustion engines applications. Appl Therm Eng 2018;133:452–63. https://doi.org/10.1016/j.applthermaleng.2017.11.131. 03/25/2018.
[60] Hemmat Esfe M, Esfandeh S, Saedodin S, Rostamian H. Experimental evaluation, sensitivity analyzation and ANN modeling of thermal conductivity of ZnO-MWCNT/EG-water hybrid nanofluid for engineering applications. Appl Therm Eng 2017;125:673–85. https://doi.org/10.1016/j.applthermaleng.2017.06.077. 10/01/2017.
[61] Hemmat Esfe M, Zabihi F, Rostamian H, Esfandeh S. Experimental investigation and model development of the

non-Newtonian behavior of CuO-MWCNT-10w40 hybrid nano-lubricant for lubrication purposes. J Mol Liq 2018;249:677–87. https://doi.org/10.1016/j.molliq.2017.11.020. 01/01/2018.

[62] Hemmat Esfe M, Saedodin S, Rejvani M, Shahram J. Experimental investigation, model development and sensitivity analysis of rheological behavior of ZnO/10W40 nano-lubricants for automotive applications. Phys E Low-dimens Syst Nanostruct 2017;90:194–203. https://doi.org/10.1016/j.physe.2017.02.015. 06/01/2017.

[63] Hemmat Esfe M, Bahiraei M, Mahian O. Experimental study for developing an accurate model to predict viscosity of CuO–ethylene glycol nanofluid using genetic algorithm based neural network. Powder Technol 2018;338:383–90. https://doi.org/10.1016/j.powtec.2018.07.013. 10/01/2018.

[64] Hemmat Esfe M, Motallebi SM. Four objective optimization of aluminum nanoparticles/oil, focusing on thermo-physical properties optimization. Powder Technol 2019;356:832–46. https://doi.org/10.1016/j.powtec.2019.08.041. 11/01/2019.

[65] Hemmat Esfe M, Abbasian Arani AA, Esfandeh S. Improving engine oil lubrication in light-duty vehicles by using of dispersing MWCNT and ZnO nanoparticles in 5W50 as viscosity index improvers (VII). Appl Therm Eng 2018;143:493–506. https://doi.org/10.1016/j.applthermaleng.2018.07.034. 10/01/2018.

[66] Alirezaie A, Saedodin S, Esfe MH, Rostamian SH. Investigation of rheological behavior of MWCNT (COOH-functionalized)/MgO - engine oil hybrid nanofluids and modelling the results with artificial neural networks. J Mol Liq 2017;241:173–81. https://doi.org/10.1016/j.molliq.2017.05.121. 09/01/2017.

[67] Hemmat Esfe M, Rostamian H, Esfandeh S, Afrand M. Modeling and prediction of rheological behavior of Al2O3-MWCNT/5W50 hybrid nano-lubricant by artificial neural network using experimental data. Phys Stat Mech Appl 2018;510:625–34. https://doi.org/10.1016/j.physa.2018.06.041. 11/15/2018.

[68] Hemmat Esfe M, Reiszadeh M, Esfandeh S, Afrand M. Optimization of MWCNTs (10%) – Al2O3 (90%)/5W50 nanofluid viscosity using experimental data and artificial neural network. Phys Stat Mech Appl 2018;512:731–44. https://doi.org/10.1016/j.physa.2018.07.040. 12/15/2018.

[69] Liu X, Mohammed HI, Ashkezari AZ, Shahsavar A, Hussein AK, Rostami S. An experimental investigation on the rheological behavior of nanofluids made by suspending multi-walled carbon nanotubes in liquid paraffin. J Mol Liq 2020;300:112269. https://doi.org/10.1016/j.molliq.2019.112269. 02/15/2020.